Journal of South American Earth Sciences 22 (2006) 89–97

Journal of
South American
Earth Sciences

www.elsevier.com/locate/jsames

3D modeling of buried intrusives in Pan de Azúcar zone (northern Puna, Argentina) from ground magnetic data

Claudia Prezzi [a,*], Hans-Jürgen Götze [b]

[a] *CONICET, Universidad de Buenos Aires, Research Fellow of the Alexander von Humboldt Foundation, Instituto de Geofísica Daniel Valencio, Dpto. de Cs. Geológicas, FCEyN, Universidad de Buenos Aires, Ciudad Universitaria, Pabellón 2, 1428 Buenos Aires, Argentina*
[b] *Institut für Geowissenschaften, Abteilung Geophysik, Christian Albrechts Universität. Otto Hahn Platz 1, 24118 Kiel, Germany*

Received 1 July 2004; accepted 1 January 2004

Abstract

The Pan de Azúcar volcanic complex crops out in the southern border of the Laguna de Pozuelos Basin and consists of several volcanic dome centers of approximately 12 Ma. The volcanic complex hosts the Pan de Azúcar mine. Previous interpretation of seismic lines north of the Pan de Azúcar outcrops has indicated the presence of buried bodies, probably related to the volcanic complex. To confirm the existence of these buried intrusives, a detailed ground magnetic survey of the southern portion of the Laguna de Pozuelos Basin (north of Pan de Azúcar) was conducted. Three-dimensional modeling of the magnetic data shows an intrusive body of approximately 1 km in diameter buried at approximate depths of 250 m. The results obtained here are valuable for further mining exploration in the area and also support the hypothesis of a large caldera buried beneath the Laguna de Pozuelos Basin.

Keywords: Ground magnetic survey; Pan de Azúcar volcanic complex; 3D magnetic modeling; Buried intrusive

---

1. Introduction

The Pan de Azúcar volcanic complex crops out in the southern border of the Laguna de Pozuelos Basin (Puna) (Fig. 1a) and consists of several volcanic dome centers of approximately 12 Ma, formed by minor intrusives, lavas, and pyroclastic rocks of dacitic composition. The basin is dominated by an extensive Quaternary cover of fluvial, playa-lake, and evaporite sediments interfingered with pyroclastic deposits.

Prior interpretations of reflection seismic lines located immediately north of Pan de Azúcar outcrops (Fig. 1b) have suggested the presence of a group of buried bodies that may be related to the volcanic complex (Gangui, 1998a). The area covered by the seismic data (recorded and processed by the YPF oil company between 1982 and 1985) corresponds to the southern part of the basin and includes six approximately E–W-trending seismic lines and two N–S cross-lines. In particular, Gangui (1998a) suggests that the east part of line 4221 (Fig. 1b) indicates the existence of buried bodies, intruding Ordovician and Tertiary sedimentary sequences, and covered by Quaternary infill.

In contrast, a regional aeromagnetic survey (Rankin and Triggs, 1997) identifies an important correspondence between dacitic dome outcrops and strong magnetic anomalies in the studied area. Chernicoff (2001), using these aeromagnetic data (see also SEGEMAR, 1996), suggests the existence of three buried subvolcanic bodies and one buried volcanic unit. Using 2.5D modeling, Chernicoff (2001) further estimates that the bodies are at depths of 120–500 m.

The determination of the existence of buried bodies in this area has two major implications. First, the volcanic complexes that outcrop in the Laguna de Pozuelos Basin are closely associated with mineralization, as part of the Bolivian tin ore polymetallic belts (Caffe et al., 2002). The well-known Pan de Azúcar Ag–Pb–Zn ore deposit (Fig. 1b), which was mined from colonial times until the

---

[*] Corresponding author. Fax: +54 11 47883439.
E-mail address: prezzi@gl.fcen.uba.ar (C. Prezzi).

0895-9811/$ - see front matter © 2006 Elsevier Ltd. All rights reserved.
doi:10.1016/j.jsames.2006.08.004

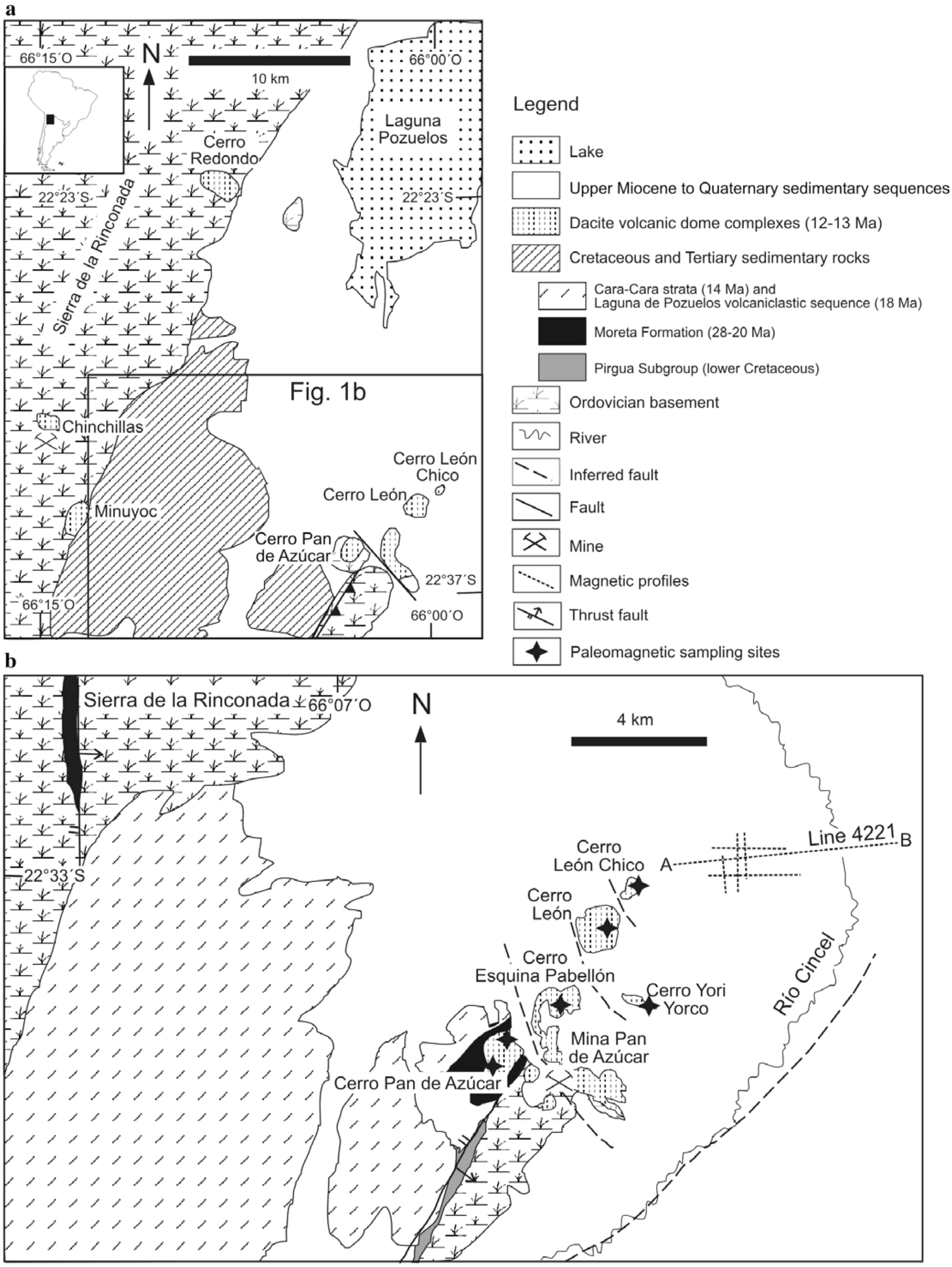

Fig. 1. (a) Simplified geologic map of Laguna de Pozuelos zone showing the location of the 12–13 Ma dacite volcanic dome complexes. Rectangle indicates the area mapped in (b). (b) Simplified geologic map of Pan de Azúcar zone. The surveyed magnetic profiles and 4221 seismic line are shown. The inferred ring fracture along the Cincel River would represent the border of the hypothetical buried, Middle Miocene, large, calderic magmatic system.

early 1990s, is situated in the Pan de Azúcar volcanic complex (Fig. 1b); the Chinchillas volcanic dome complex (Fig. 1a) hosts a mineralized hydrothermal breccia (Pb–Zn–Sn) that has been mined intermittently (Caffe et al., 2002); and the Cerro Redondo volcanic complex (Fig. 1a) hosts the mining prospect Cerro Redondo (Ag–Zn–Pb–Cu) (Caffe and Coira, 1999).

Second, different authors (Coira, 1979; Chernicoff et al., 1996; Coira et al., 1996; Coira and Caffe, 1999) have suggested the existence of a large ancient caldera (Miocene) beneath the central and southern part of the Laguna de Pozuelos Basin, covered by the infilling sediments. Coira et al. (1996) propose that the dome volcanic complexes (Cerro Redondo, Chinchillas, Pan de Azúcar) (Fig. 1a) may represent the final stages of such a calderic magmatic system. The most important pieces of evidence to support such a hypothesis are as follows: the curvature of the Cincel River, which is supposed to follow a large-scale ring fracture (Fig. 1b); the existence of pyroclastic sequences (20–12 Ma) along the inferred fracture; the change in trend from N–S to NE-SW of the faults that correspond to the eastern boundaries of the Sierras de Cochinoca and Quichagua, respectively; and the aeromagnetic anomalies identified in the area by Chernicoff et al. (1996).

Thus, the determination of the existence, 3D shape, depth, and size of buried dacite bodies would be of interest not only for future mining explorations of this zone but also to confirm the presence of the buried magmatic system. The identification of such a large Middle Miocene caldera would bring new insight into the magmatic evolution of the northern Puna.

In light of the preceding information and to confirm the existence of buried intrusives, a detailed ground magnetic survey of the Laguna de Pozuelos area (north of Pan de Azúcar) was conducted (Prezzi, 2002). Through 3D modeling of the detected anomalies, the existence of a body of nearly 1 km^3 volume, buried at depths between 150 and 350 m, has been determined.

2. Geologic setting

The Laguna de Pozuelos (Fig. 1a) is located in northern Puna. This 100 km long, 20 km wide depression corresponds to an internally drained basin. Its western boundary is represented by the Sierra de la Rinconada (Fig. 1a). The oldest outcropping units correspond to the Ordovician Acoite Formation and consist of marine shales and thin-bedded sandstones (Figs. 1a, b). Small outcrops of Lower Cretaceous sediments of the Pirgua Subgroup (Coira, 1979) are mapped to the south of the area (Fig. 1b). Main outcrops of Cenozoic sedimentary successions include at least four pre-Upper Miocene units. The 28–20 Ma Moreta Formation (Coira, 1979; Linares and González, 1990) is a conspicuous, coarse-grained intramontane infilling, similar to those formed contemporaneously in the Bolivian Eastern Cordillera (Kley et al., 1996). The Moreta Formation rocks are followed by the Laguna de Pozuelos volcaniclastic sequence (18.6 ± 1 Ma; Caffe et al., 2002), which comprises alternating pyroclastic and reworked volcanic rocks that crop out in the southwestern border of the Laguna de Pozuelos Basin (Fig. 1b). It underlies mid-Miocene sediments and tuffs of the Cara Cara strata dated at 14.26 ± 0.19 Ma (Cladouhos et al., 1994). A group of three volcanic dome complexes postdates the latter sequences and are described in the following sections.

2.1. Pan de Azúcar (22°36′S; 66°03′W)

The Pan de Azúcar volcanic dome complex (Fig. 1b) is composed of lava domes, lava flows, and a group of pyroclastic units erupted from several associated vents in the southern portion of the Laguna de Pozuelos Basin (Fig. 1b). It consists of different dacite domes: Pan de Azúcar, Esquina Pabellón, Cerro León Grande, León Chico, and Cerro Yori Yorco (Fig. 1b). The center hosts an important Pb–Zn–Ag (±Sn) ore deposit. Dacitic rocks cover the Ordovician basement, as well as Moreta Formation rocks and Cara Cara strata. Available K–Ar ages from Pan de Azúcar rocks (12 ± 2 Ma, 13 ± 1 Ma; Coira, 1979; Linares and González, 1990) indicate the complex may be situated within the late Middle Miocene. Volcanic activity in the region was favored by NW-SE-trending fractures (Coira, 1979; Coira et al., 1996). Such fractures would be related to strike-slip movements along the major faults that bound the Laguna de Pozuelos Basin (Coira et al., 1996).

2.2. Cerro Redondo (22°22′S; 66°08′W)

This volcanic dome complex crops out in the eastern border of the Sierra de Rinconada (Fig. 1a), directly overlying the Ordovician basement (Acoite Formation). The only available radiometric date of 12.54 ± 1.1 Ma (apatite fission track) was obtained by Cladouhos et al. (1994). The eruptive history started with the deposition of a thick volcanic breccia-block and ash succession, followed by dacitic lava domes set through a group of nested ring fractures (Caffe, 1999). This volcanic complex hosts the mining prospect Cerro Redondo (Ag–Zn–Pb–Cu) (Caffe and Coira, 1999).

2.3. Chinchillas (22°30′S; 66°15′W)

The Chinchillas volcanic dome complex (Fig. 1a) is a small volcanic center located inside the Sierra de Rinconada. The complex has been dated by a single K–Ar age determination of 13 ± 1 Ma (Linares and González, 1990). The center is set over the Ordovician Acoite Formation and comprises massive, low-volume, pyroclastic flow deposits, block and ash flow deposits, and a dacite lava dome. Similar to Pan de Azúcar, this volcanic structure erupted along a NW–SE fracture system related to strike-slip movements along the fault that bounds the Sierra de la Rinconada on the east (Coira et al., 1996). This volcanic dome complex hosts a mineralized hydrothermal breccia (Pb–Zn–Sn) that has been mined intermittently (Caffe et al., 2002).

3. Methodology

The ground magnetic survey was conducted using a Scintrex ENVI MAG proton magnetometer. The location of each station was determined using GPS. The total magnetic field was measured on 637 stations along six profiles, three trending approximately N–S and three trending approximately E–W (Fig. 1b). The distance between stations was 25 m. The profile AB (6.7 km length), which runs along the central section of the 4221 seismic line (Fig. 1b), was surveyed first to determine the existence and location

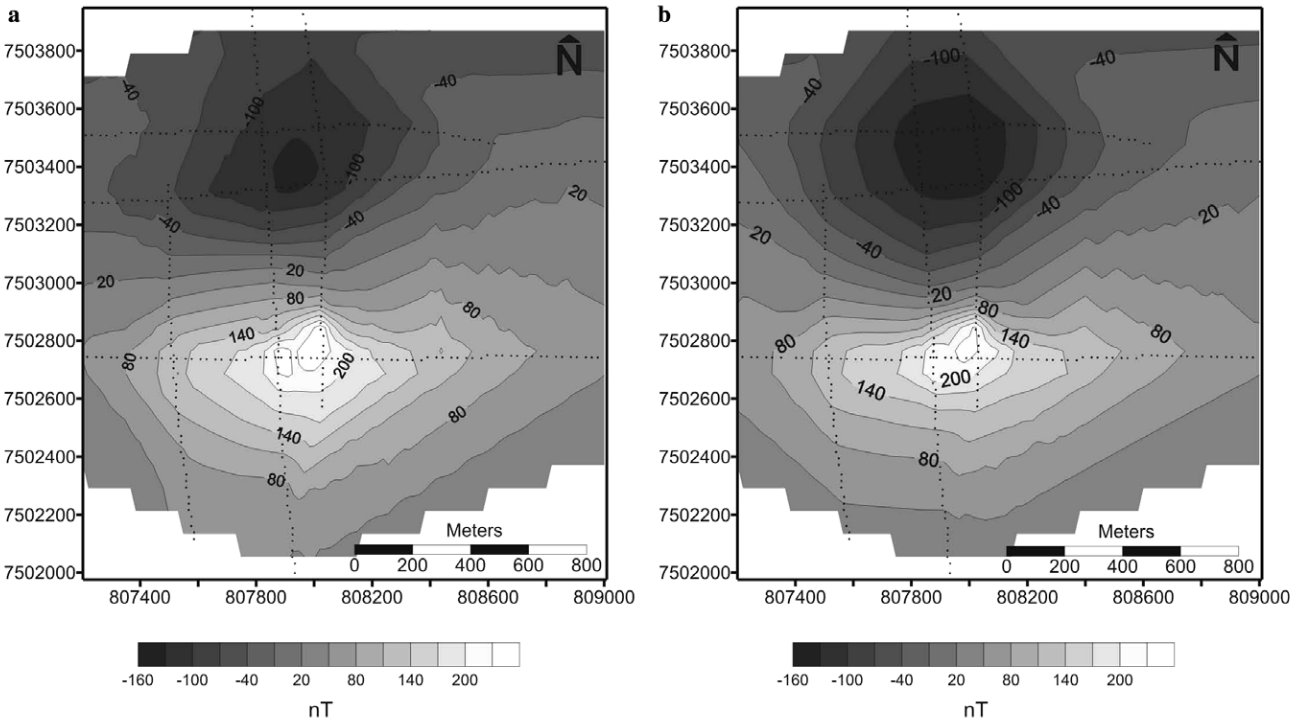

Fig. 2. (a) Measured and (b) modeled anomalies. A reverse dipolar magnetic anomaly with a minimum of −150 nT in the northern sector and a maximum of 250 nT in the southern sector is observed. Each dot corresponds to a measured station.

Table 1
Magnetic parameters used in the model

	Natural remanent magnetization			Susceptibility 10^{-5} SI	Könisberg ratio
	Declination	Inclination	Intensity		
Dacite dome	175°	35°	4.42 A/m	337	70
Sedimentary sequences	0°	−39°	0.0017 A/m	0.62	14.4

Table 2
Magnetic parameters from previous paleomagnetic study (Prezzi et al., 2004)

Site	Location		Natural remanent magnetization					Susceptibility 10^{-05} SI	Könisberg ratio
	Latitude	Longitude	$n(n_c)$	D	I	α_{95}	Intensity		
Cerro León Chico dacitic dome	22° 33.5′S	66°01′W	15(9)	177.2°	42.4°	4.2°	3.13	337.3	50.2
Cerro León Grande dacitic dome	22°34′S	66°02.5′W	9(7)	247.8°	59.8°	29.9°	3.06	1368.9	11.9
Cerro Yori Yorco dacitic dome	22°35′S	66°01.6′W	13(12)	14.2°	−43.9°	14.9°	0.2	695.2	1.6
Cerro Esquina Pabellón dacitic dome	22°35.2′S	66°03.3′W	13(12)	21.1°	−51.9°	18.2°	0.025	101.9	1.3
Cerro Pan de Azúcar dacitic dome – Site A	22°37′S	66°04.5′W	21(18)	0.2°	−41.4°	3.1°	0.57	112.8	27.3
Cerro Pan de Azúcar dacitic dome – Site B	22°36′S	66°04′W	11(10)	20.9°	53°	76.8°	0.037	25.6	7.8

Notes. $n(n_c)$ is number of specimens used in statistic (number of samples collected), D and I are declination and inclination of the mean direction of the natural remanent magnetization, and α_{95} is the semiangle of the 95% confidence cone about the mean direction of the natural remanent magnetization. Intensity in A/m.

of possible magnetic anomalies associated with the buried magmatic bodies interpreted by Gangui (1998a,b). The body modeled here corresponds to the westernmost one identified by Gangui (1998a,b) along this seismic line. The other profiles are between 1.2 and 2.8 km long and approximately parallel and perpendicular to a section of profile AB along which anomalous values of the Earth's magnetic field were detected (Fig. 1b). The bulk magnetic susceptibility of the different formations is known from previous studies (Rankin and Triggs, 1997; Prezzi et al., 2001, 2004).

The measured values were corrected according to diurnal variation of the Earth's magnetic field. Diurnal variation was recorded by measuring the total magnetic field in the base station (located using GPS) approximately every 50 min. The diurnal variation was approximately

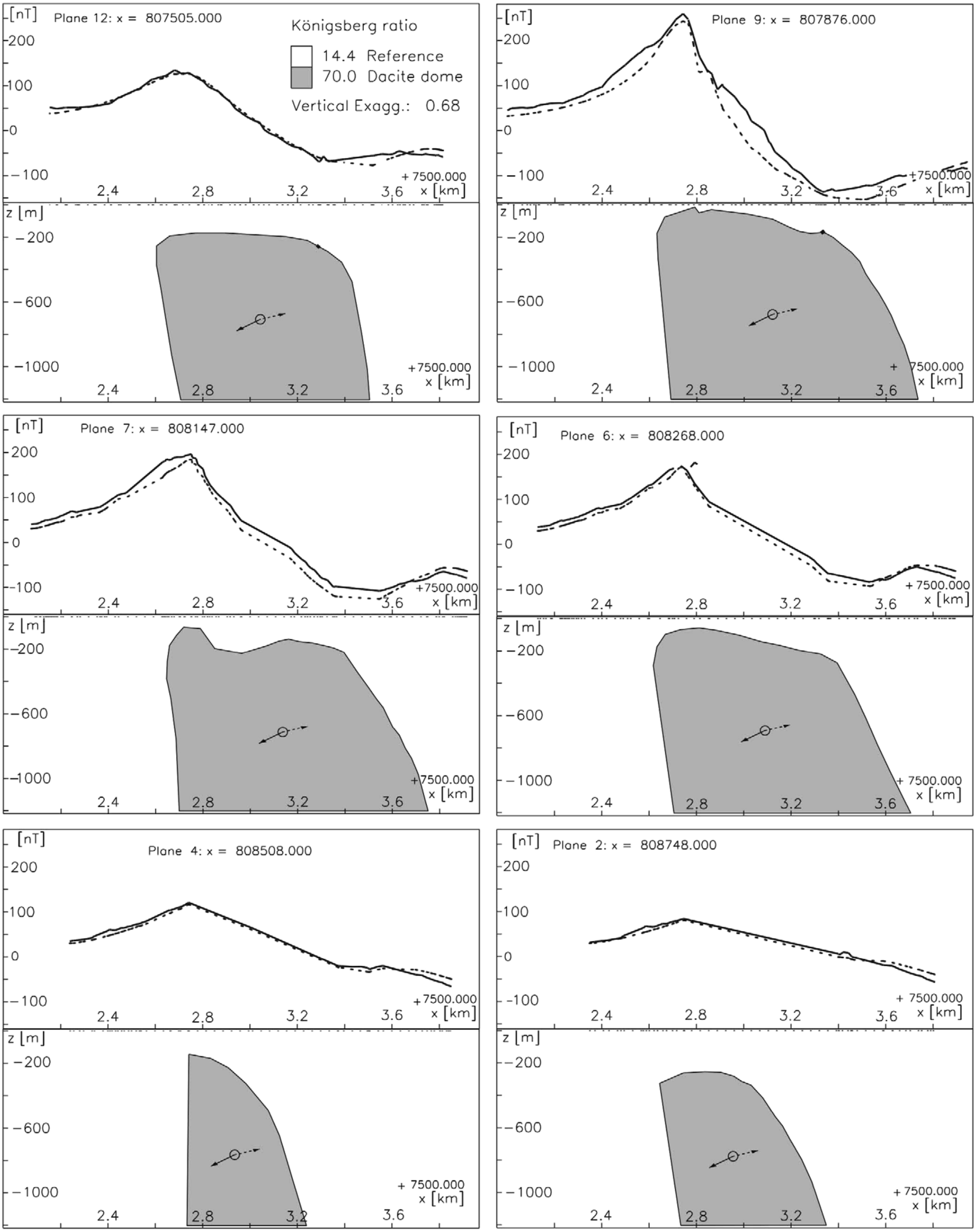

Fig. 3. Comparison between measured and modeled anomalies along some of the modeled vertical planes. Solid (dashed) line: measured (calculated) anomaly. Solid (dashed) arrows: remanent (induced) magnetization of the modeled body. Reference: Ordovician, Tertiary, and Quaternary sedimentary sequences.

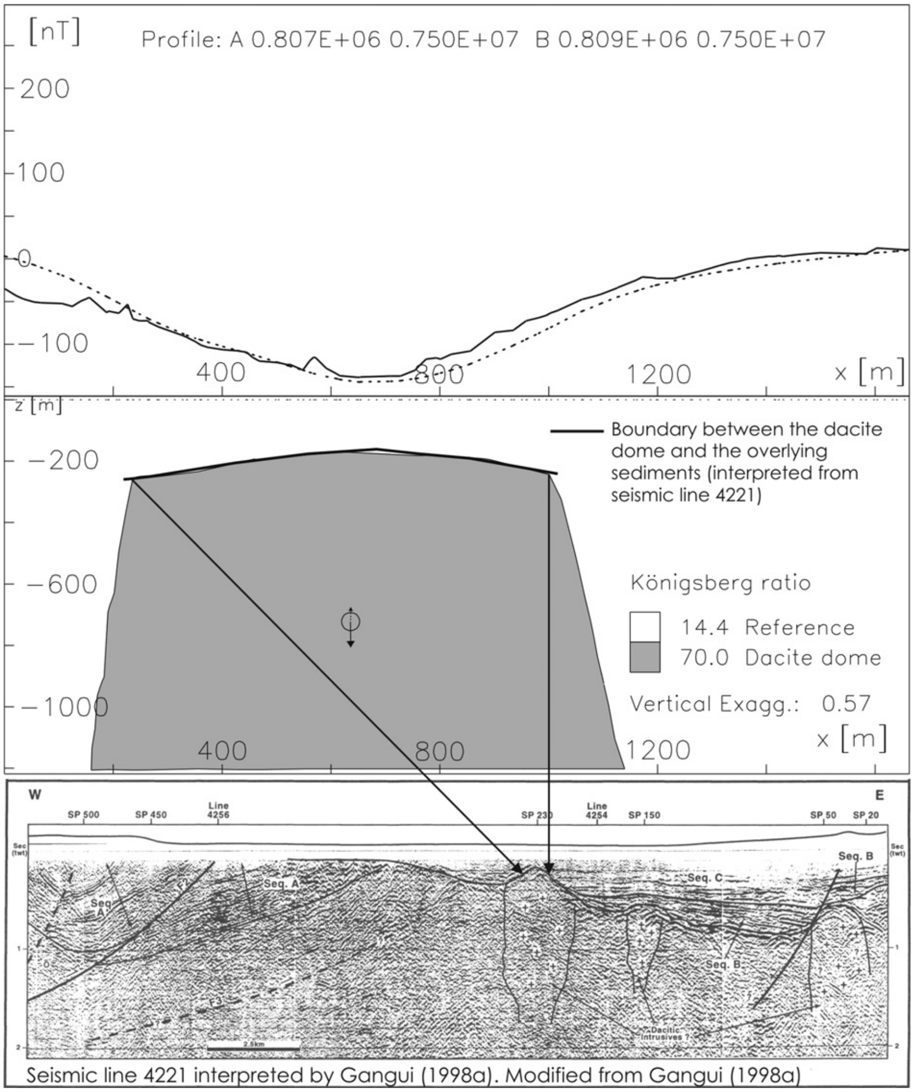

Fig. 4. Comparison between measured and modeled anomalies for a vertical cross-section along seismic line 4221. A good fit can be observed between the depths to the top of the body obtained through magnetic modeling and those calculated from seismic data. Solid (dashed) line: measured (calculated) anomaly. Solid (dashed) arrows: remanent (induced) magnetization of the modeled body. Reference: Ordovician, Tertiary, and Quaternary sedimentary sequences.

50 nT in this area during the survey. The value of the International Geomagnetic Reference Field (corresponding to May 2000) was subtracted from the corrected data.

The resulting anomalies were modeled by the interactive modeling tool IGMAS (Götze and Lahmeyer, 1988), which stands for ‘‘interactive gravity and magnetic application system’’ and uses triangulated polyhedrons to approximate areas of constant density and/or susceptibility within the Earth’s crust and mantle. The automated triangulation of model surfaces is defined through a series of parallel, vertical cross-sections that enable the user to construct even complicated model geometries. The numerical algorithms were developed by one of the authors (Götze, 1984) and allow for the calculation of geoid, gravity field, and gradients, as well as magnetic field components and components of remnant and induced magnetic fields in one program step. The IGMAS software package thus eases 3D interpretations of gravity and magnetic databases; it also provides a wide range of GIS functions in 3D space (e.g., data queries, interoperability, visualization, interdisciplinary interpretations in an object-oriented data environment) to integrate other geophysical models, information, and data from both geophysics and geology (Schmidt and Götze, 1998, 1999; Breunig et al., 2000; Götze and Schmidt, 2002; see also http://www.geophysik.uni-kiel.de/~sabine/Sabine_IGMAS.html).

The 3D model is partially constrained by the reflection seismic data mentioned previously. The location of the top of the buried body interpreted by Gangui (1998a,b) along the 4221 seismic line was converted from two-way travel time to depth using a constant velocity of 1.528 km/s. This velocity was chosen on the basis of the age, type of rocks, and average travel times to such interfaces.

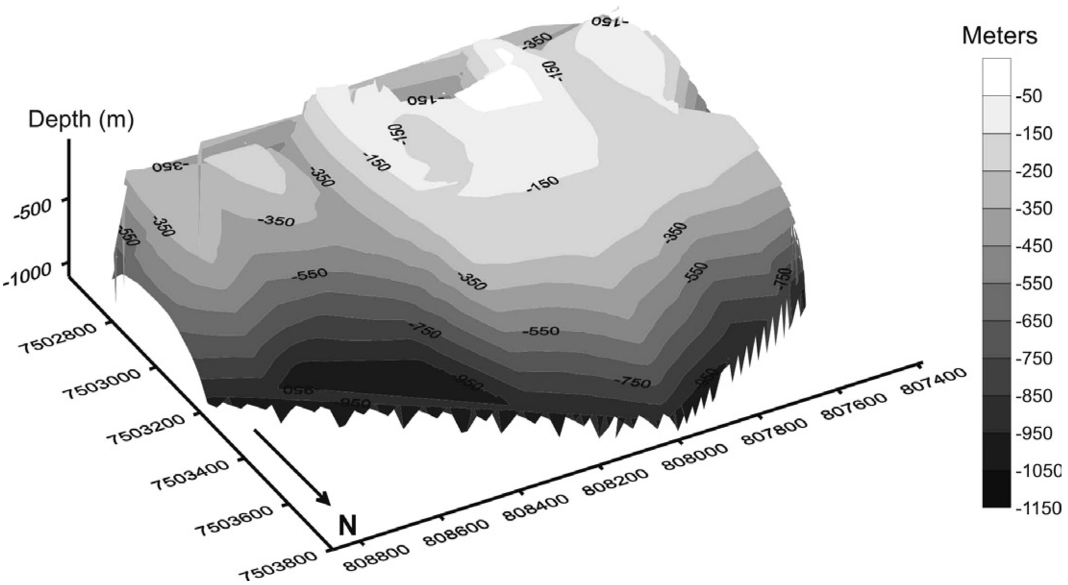

Fig. 5. Three-dimensional plot showing the location, 3D shape, size, and depth beneath the surface of the top of the modeled buried dacite dome.

4. Results

The magnetic anomaly map (Fig. 2a) shows the existence of a dipolar reverse anomaly with a minimum of −150 nT in the northern sector and a maximum of 250 nT in the southern sector. The 3D modeling was performed along 13 N–S vertical modeling planes, spaced at approximately 120 m intervals. Fig. 2b presents the modeled magnetic anomaly. The correlation coefficient between the measured and modeled anomalies is 0.98, and the standard deviation of the residual anomaly is 19.8. To generate the modeled anomaly, the presence of strong, reverse natural remanent magnetization in the buried dacite body was taken into account. Similar values to those reported for Cerro León Chico in previous paleomagnetic studies (Prezzi et al., 2001, 2004) were used (Tables 1 and 2, Fig. 1). Some of the vertical planes modeled are shown in Fig. 3.

A vertical cross-section along seismic line 4221 is presented in Fig. 4. A good fit can be observed between the depths to the top of the buried body, obtained through forward modeling of the magnetic data, and those calculated from Gangui's (1998a,b) interpretations of the seismic data.

The 3D modeling confirms the existence of a simple body, approximately 1 km in diameter, with a minimum average depth of nearly 150 m beneath the surface, and an estimated volume of 1.02 km^3. The 3D shape, size, location, and depth of this body can be observed in Fig. 5.

5. Discussion and conclusions

This study demonstrates that in the case of the dacitic volcanic complexes, an understanding of the natural remanent direction within and around the intrusive can play a significant role in the interpretation of magnetic anomalies. This fact should be taken into account when interpreting magnetic data from northern Puna–Cordillera Oriental. Remanent magnetization has been documented and considered in the analysis of magnetic anomalies only rarely, possibly because the remanent component is generally small compared with the induced one. Furthermore, the measurement of remanence requires specialized field sampling and laboratory techniques.

The 3D magnetic modeling carried out here indicates the existence of a buried intrusive immediately north of Pan de Azúcar volcanic complex. The estimation of the 3D shape, size, and depth of this body is valuable for future mining explorations of the area, in that the Pan de Azúcar ore deposit was mined up to a depth of 250 m.

Moreover, the results support the hypothesis of a large caldera buried beneath the central and southern sectors of Laguna de Pozuelos Basin. The buried body modeled in this study is located northeast of Cerro León Chico (Fig. 6), which suggests that the dome complexes of Laguna Pozuelos may lie along a ring fracture associated with the Cincel River (Fig. 6). Such a fracture would represent the edge of the large buried calderic magmatic system. It is generally accepted that the northern Puna is characterized by a virtual Late Oligocene–Middle Miocene volcanic quiescence. Volcanism began at 14–10 Ma but was restricted to stocks and domes. Voluminous ignimbrites sheets erupted from huge calderas only after 10 Ma (e.g., Coira and Caffe, 1999; Kay et al., 1999), so the existence of a large Middle Miocene caldera would have important implications for the magmatic evolution of this region.

Regarding the mining potential of the area, new prospects might arise in other sectors where buried bodies associated with the large caldera border ring fractures also might exist. The possible presence of another buried body

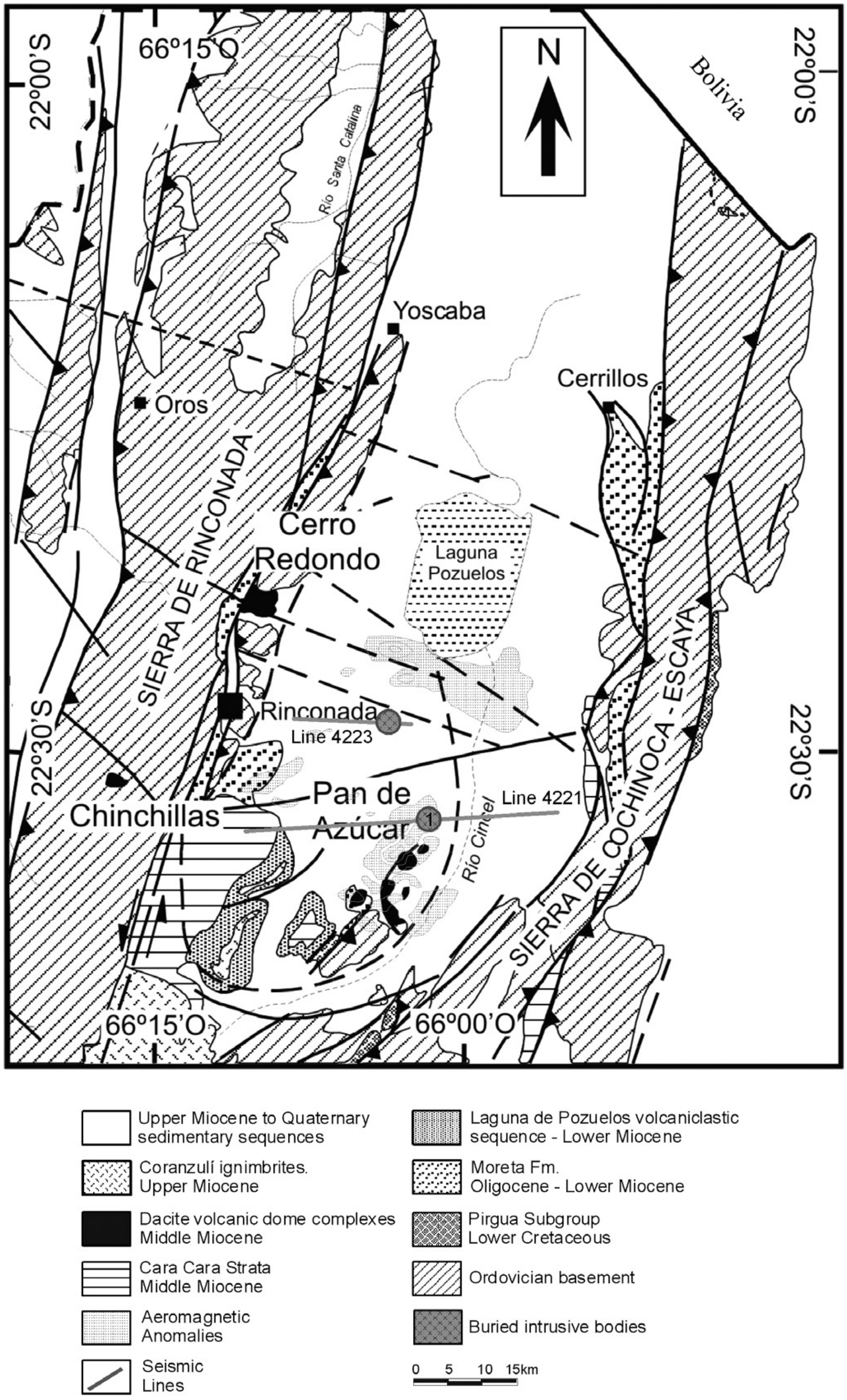

Fig. 6. Geologic map (modified from Prezzi et al., 2004) showing the inferred ring fracture that would represent the edge of the large, buried, calderic magmatic system; the location of buried intrusive bodies interpreted from seismic lines 4221 and 4223 by Gangui (1998a) and modeled in this study (body 1); and the aeromagnetic anomalies detected in the area (Chernicoff et al., 1996).

has been indicated by Gangui (1998a) along a seismic line approximately 9.5 km north of the intrusive detected here (line 4223) (Fig. 6). Chernicoff (2001) has suggested the existence of other two volcanic intrusives north of this seismic line according to 2.5D aeromagnetic data modeling (Fig. 6). Considering these interpretations and the results obtained herein, it would be useful to carry out a detailed ground magnetic and gravimetric survey north of the studied area.

Acknowledgements

The authors especially thank Dr. Beatriz Coira, Hernán Justi, and Roberto Rojas for their help in the fieldwork and logistical support. C. Prezzi gratefully acknowledges the support of an Alexander von Humboldt Research Fellowship from the Alexander von Humboldt Foundation. Financial support for this work was received from Agencia Nacional de Promoción Científica y Tecnológica (ANPCyT) (Project BID1201/OC-AR-PICT2003-07-13551).

References

Breunig, M., Cremers, A.B., Götze, H.-J., Seidemann, R., Schmidt, S., Shumilov, S., Siehl, A., 2000. Geologic mapping based on 3D models using an interoperable GIS. GIS – Journal for Spatial Information and Decision Making 13 (2), 12–18.

Caffe, P.J., 1999. Complejos volcánicos dómicos del Terciario superior de Puna Norte: sus implicancias magmatotectónicas y metalogenéticas. PhD Thesis. Facultad de Ciencias Exactas, Físicas y Naturales, Universidad Nacional de Córdoba, Argentina, 421pp. (unpublished).

Caffe, P., Coira, B., 1999. Complejos de domos volcánicos del Mioceno medio de Puna Norte. Un modelo geológico y metalogenético para yacimientos epitermales de metales de base ricos en Ag (Sn). In: Zappettini, E. (Ed.), Recursos minerales de la República Argentina. Instituto de Recursos Minerales, SEGEMAR, Buenos Aires, Argentina. Anales 35, 1569–1578.

Caffe, P.J., Trumbull, R.B., Coira, B.L., Romer, R.L., 2002. Petrogenesis of Early Neogene magmatism in the Northern Puna; implications for magma genesis and crustal processes in the Central Andean Plateau. Journal of Petrology 43, 907–942.

Chernicoff, C., 2001. Evidencias geofísicas de la continuidad del volcanismo dacítico mioceno en el subsuelo de la depresión de Pozuelos, provincia de Jujuy, y su potencialidad minera. Revista de la Asociación Geológica Argentina 56 (4), 517–528.

Chernicoff, C., Garea, G., Rankin, L., Zappettini, E., 1996. Interpretación geológica del relevamiento aeromagnético de la Puna Septentrional, Jujuy y Salta. Área depresión de Pozuelos, Geofísica. Dirección Nacional del Servicio Geológico, Serie Contribuciones Técnicas-Geofísica, vol. 1, pp. 14–17. Buenos Aires.

Cladouhos, T.T., Allmendinger, R.W., Coira, B., Farrar, E., 1994. Late Cenozoic deformation in the Central Andes: fault kinematics from the northern Puna, northwestern Argentina and southwestern Bolivia. Journal of South American Earth Sciences 7 (2), 209–228.

Coira, B., 1979. Descripción geológica de la Hoja 3c, Abra Pampa, Provincia de Jujuy. Servicio Geológico Nacional, Buenos Aires. Boletín 170, 90pp.

Coira, B., Caffe, P., 1999. Volcanismo Cenozoico de Puna Norte. In: González Bonorino G., Omarini, R., Viramonte, J. (Eds.), Geología del Noroeste Argentino. Relatorio 14° Congreso Geológico Argentino, Salta, vol. 1, pp. 371–386.

Coira, B., Caffe, P., Soler, M., 1996. Interpretación geológica del relevamiento aeromagnético de la Puna Septentrional, Jujuy y Salta. Área depresión de Pozuelos, Geología y Minería. Dirección Nacional del Servicio Geológico, Serie Contribuciones Técnicas-Geofísica, vol. 1, pp. 11–13. Buenos Aires.

Gangui, A., 1998a. A combined structural interpretation based on seismic data and 3-D gravity modeling in the Northern Puna/Eastern Cordillera, Argentina. Berliner Geowissenschaftliche Abhandlungen (B)27, 176pp. Berlin, Alemania.

Gangui, A., 1998b. Seismic stratigraphy of the Pozuelos basin, Northern Puna, Argentina. Actas 10° Congreso Latinoamericano de Geología y 6° Congreso Nacional de Geología Económica, vol. 1, pp. 12–17. Buenos Aires, Argentina.

Götze, H.-J., 1984. Über den Einsatz interaktiver Computergraphik im Rahmen 3-dimensionaler Interpretationstechniken in Gravimetrie und Magnetik. Habil. Schrift, Techn. Univ. Clausthal, 236 Seiten, unveröffentlicht.

Götze, H.-J., Lahmeyer, B., 1988. Application of three-dimensional interactive modeling in gravity and magnetics. Geophysics 53 (8), 1096–1108.

Götze, H.-J., Schmidt, S., 2002. Geophysical 3D Modeling using GIS-Functions. In 8th Annual Conference of the International Association for Mathematical Geology. ISSN: 0946-8978, Terra Nostra, Heft 04/2002, pp. 87–92.

Kay, S., Mpodozis, C., Coira, B., 1999. Magmatism, tectonism, and mineral deposits of the Central Andes (22°-33°S latitude). In: Skinner, B. (Ed.), Geology and Ore Deposits of the Central Andes. Society of Economic Geology Special Publication (SEG), vol. 7, pp. 27–59.

Kley, J., Muller, J., Tawackoli, S., Jacobshagen, V., Manutsoglu, E., 1996. Pre-Andean and Andean-age deformation in the Eastern Cordillera of Southern Bolivia. Journal of South American Earth Sciences 10, 1–19.

Linares, E., González, R.R., 1990. Catálogo de edades radiométricas de la República Argentina 1957–1987. Asociación Geológica Argentina, Publicaciones Especiales, vol. 19, 628pp.

Prezzi, C., 2002. Relevamiento magnetométrico terrestre de la zona de Pan de Azúcar, Puna Jujeña (22°30′S–66°00′O). Revista de la Asociación Geológica Argentina 57 (1), 85–91.

Prezzi, C., Somoza, R., Caffe, P., Coira, B., 2001. Estudio paleomagnético de la zona de Laguna Pozuelos (Puna Jujeña), Argentina: ausencia de rotaciones según ejes verticales. XI Congreso Latinoamericano de Geologia. Montevideo, Uruguay.

Prezzi, C., Caffe, P., Somoza, R., 2004. New paleomagnetic data from the northern Puna and western Cordillera Oriental, Argentina: a new insight on the timing of rotational deformation. Journal of Geodynamics 38, 93–115.

Rankin, L., Triggs, D., 1997. Area de la Puna Argentina. Interpretación geológica de datos de geofísica aérea y Landsat TM. SEGEMAR, Subsecretaría de Minería, República Argentina, 41pp. Buenos Aires.

Schmidt, S., Götze, H.-J., 1998. Interactive visualization and modification of 3D models using GIS functions. Physics and Chemistry of the Earth 23 (3), 289–295.

Schmidt, S., Götze, H.-J., 1999. Integration of data constraints and potential field modelling – an example from southern Lower Saxony, Germany. Physics and Chemistry of the Earth (A) 24 (3), 191–196.

SEGEMAR, 1996. Levantamiento geofísico aéreo (magnetometría y espectrometría de rayos gammas) Area Puna Septentrional. Datos Digitales. Servicio Geológico Minero Argentino.